Effect of Tumor Microenvironment Modulation on the Efficacy of Oncolytic Virus Therapy

Kazuhiko Kurozumi, Jayson Hardcastle, Roopa Thakur, Ming Yang, Gregory Christoforidis, Giulia Fulci, Fred H. Hochberg, Ralph Weissleder, William Carson, E. Antonio Chiocca, Balveen Kaur

Background The tumor microenvironment is being increasingly recognized as an important determinant of tumor progression as well as of therapeutic response. We investigated oncolytic virus (OV) therapy–induced changes in tumor blood vessels and the impact of modulating tumor vasculature on the efficacy of oncolytic virus therapy.

Methods Rat glioma cells (D74/HveC) were implanted intracranially in immune-competent rats. Seven days later, the rats (groups of 3–7 rats) were treated with oncolytic virus (hrR3), and, 3 days later, brains were harvested for evaluation. Some rats were treated with angiostatic cRGD peptide 4 days before oncolytic virus treatment. Some rats were treated with cyclophosphamide (CPA), an immunosuppressant, 2 days before oncolytic virus treatment. Changes in tumor vascular perfusion were evaluated by magnetic resonance imaging of live rats and by fluorescence microscopy of tumor sections from rats perfused with Texas red–conjugated lectin immediately before euthanasia. Leukocyte infiltration in tumors was evaluated by anti-CD45 immunohistochemistry, and the presence of oncolytic virus in tumors was evaluated by viral titration. Changes in cytokine gene expression in tumors were measured by quantitative real-time polymerase chain reaction–based microarrays. Survival was analyzed by the Kaplan–Meier method. All statistical tests were two-sided.

Results Oncolytic virus treatment of experimental rat gliomas increased tumor vascular permeability, host leukocyte infiltration into tumors, and intratumoral expression of inflammatory cytokine genes, including interferon gamma (IFN-γ). The increase in vascular permeability was suppressed in rats pretreated with cyclophosphamide. Compared with rats treated with hrR3 alone, rats pretreated with a single dose of cRGD peptide before hrR3 treatment had reduced tumor vascular permeability, leukocyte infiltration, and IFN-γ protein levels (mean IFN-γ level for hrR3 versus hrR3 + cRGD = 203 versus 65.6 μg/mg, difference = 137 μg/mg, 95% confidence interval = 72.7 to 202.9 μg/mg, $P = .006$); increased viral titers in tumor tissue; and longer median survival (21 days versus 17 days, $P<.001$).

Conclusions A single dose of angiostatic cRGD peptide treatment before oncolytic virus treatment enhanced the antitumor efficacy of oncolytic virus.

J Natl Cancer Inst 2007;99:1768–81

The tumor microenvironment plays a key role in controlling the growth and spread of solid tumors (1). Considering the complicated interplay between cancer cells and their microenvironment, it is not surprising that most therapeutic strategies aimed at treating either malignant cells themselves or their microenvironment alone have demonstrated only modest efficacy in clinical trials (2).

Malignant gliomas remain a challenging tumor to treat, and a variety of experimental therapies have failed to show effectiveness in clinical trials [reviewed in (3)]. One hallmark of malignant gliomas is the initiation of neoangiogenesis and vasculogenesis, which are consequences of disruptions in the normal homeostasis between angiogenic and antiangiogenic factors (4–7). The resulting vasculature is characterized by tortuous vessels that feature disruptions in their structural integrity, increased leakiness, uneven focal thickness, and arteriovenous shunts not seen in normal brain vasculature. Excessive endothelial cell proliferation in glioma leads to the formation of proliferating endothelial cell aggregates called glomeruloid bodies. All of these changes in tumor vasculature lead to increased thrombotic events and irregular circulation compared

Affiliations of authors: Dardinger Laboratory for Neuro-oncology and Neurosciences, Department of Neurological Surgery (KK, JH, RT, EAC, BK), Integrated Biological Graduate Program of Studies (JH), and Departments of Radiology (MY, GC) and Surgery (WC), James Comprehensive Cancer Center, The Ohio State University Medical Center, Columbus, OH; Center for Molecular Imaging Research (RW) and Department of Neurology (FHH), Massachusetts General Hospital, Charlestown, MA; Department of Neurosurgery, Brain Tumor Research Center, Massachusetts General Hospital, Boston, MA (GF).

Correspondence to: Balveen Kaur or E. Antonio Chiocca, Dardinger Laboratory for Neuro-oncology and Neurosciences, Department of Neurological Surgery, The Ohio State University, 385-D OSUCCC, 410 West 12th Ave, Columbus, OH 43210 (e-mail: balveen.kaur@osumc.edu or ea.chiocca@osumc.edu).

See "Funding" and "Notes" following "References."

DOI: 10.1093/jnci/djm229

with that in the corresponding normal brain [for review, see (7,8)]. This abnormal circulation causes an increase in the interstitial fluid pressure and a reduction in tumor oxygenation, which together pose a substantial barrier to radiation and chemotherapy (9).

Oncolytic viruses (OVs) are a biologic therapeutic approach to treating cancer that employs attenuated strains of viruses whose replication and cytotoxicity are limited to tumor cells. A variety of such viruses have been tested in vitro and in animal models, and some have reached testing in clinical trials [for review, see (10)]. Although published clinical trials of oncolytic virus therapy have not revealed evidence of dose-related toxicities, they have also not revealed convincing evidence of efficacy. The inability to translate the tumor-killing properties achieved by oncolytic viruses in experimental models into effective "cures" in patients has led us to hypothesize that changes in the tumor microenvironment in response to ongoing oncolysis may limit the therapeutic effectiveness of oncolytic viruses.

Although the impact of host defense mechanisms on limiting oncolytic virus propagation in tumors is being recognized (11,12), the effect of oncolytic virus infection on tumor vasculature has not, to our knowledge, been examined in detail. Here, we analyzed the changes in vascular hyperpermeability in intracerebral tumors treated with oncolytic virus relative to phosphate-buffered saline (PBS)–treated control tumors in a syngeneic rat brain tumor model. We further tested the effect of activated endothelium on oncolytic virus–induced inflammation by using antiangiogenic treatment with cyclic RGD (cRGD) peptide before oncolytic virus therapy in a rat glioma model (13). cRGD peptide is an integrin antagonist and an antiangiogenic agent that has shown efficacy in glioblastoma growth in animals (13). It is currently being evaluated in phase II clinical trials for safety and efficacy against newly diagnosed and recurrent glioblastoma multiforme. Results from a multi-institutional phase I trial in patients with recurrent malignant glioma have shown that cRGD peptide is well tolerated at a maximum dose of 2400 mg/m^2 (14). Durable complete and partial responses observed in this study were related to changes in the relative cerebral blood flow in these patients (14).

CONTEXT AND CAVEATS

Prior knowledge

Oncolytic viruses have tumor-killing properties in experimental models but have not shown convincing evidence of efficacy in patients. Innate host immune responses combined with changes in the tumor microenvironment in response to ongoing oncolysis may limit the therapeutic effectiveness of oncolytic viruses. Tumor vasculature is a major determinant of tumor microenvironment, and we hypothesized that changes in tumor vascular perfusion would affect therapeutic outcome.

Study design

In vivo study of oncolytic virus therapy–induced changes in tumor blood vessels and the impact of modulating tumor vasculature on the efficacy of oncolytic virus therapy in a rat glioma model.

Contribution

Oncolytic virus treatment of rat gliomas increased the permeability of the tumor vasculature, tumor inflammation, and leukocyte infiltration. Pretreatment of gliomas with an angiogenesis inhibitor reduced inflammation, vascular hyperpermeability, and leukocyte infiltration of tumor tissue upon treatment with oncolytic virus and enhanced the anticancer efficacy of oncolytic virus treatment by increasing oncolytic virus propagation in tumors.

Implications

The use of antiangiogenic agents may improve the efficacy of oncolytic virus in patients.

Limitations

The effect of antiangiogenic agents on the efficacy of oncolytic viral therapy in a human glioma model in athymic nude mice is not known. The increased viral replication supported by tumors pretreated with antiangiogenic agents could lead to toxic effects that are associated with increased viral burden.

Materials and Methods

Viruses and Cell Lines

hrR3 is an oncolytic virus that was derived from type 1 herpes simplex virus (HSV-1) by insertion of the LacZ gene into the HSV-1 UL39 locus, which inactivates the viral ICP6 gene (15). rHSVQ is an HSV-1–derived recombinant oncolytic virus that has a disrupted UL39 locus and carries deletions in both copies of the γ34.5 gene (16). Viral stocks were generated in Vero African green monkey kidney cells (American Type Culture Collection, Manassas, VA) as previously described (17). Rat glioma D74/HveC cells (kindly provided by E. A. Chiocca, The Ohio State University, Columbus, OH) were grown in Dulbecco's modified Eagle Medium (DMEM) supplemented with 10% fetal bovine serum, 2 mM glutamine, 100-U/mL penicillin, 100-μg/mL streptomycin, and 7.5-μg/mL blasticidin S (Calbiochem/Emanuel Merck Dermstadt (EMD) Biosciences, La Jolla, CA) as described (17). Human U87ΔEGFR glioma cells (kindly provided by H. J. Huang and W. K. Cavenee, Ludwig Institute for Cancer Research, San Diego CA), which are stably transfected with a plasmid that expresses a constitutively active mutant form of epidermal growth factor receptor (EGFR) (18), were maintained in DMEM supplemented with 10% fetal bovine serum, 2 mM glutamine, 100-U/mL penicillin, 100-μg/mL streptomycin, and 200-μg/mL G418 (Sigma-Aldrich, St Louis, MO).

Animal Studies

All animal experiments were performed according to the guidelines of the Subcommittee on Research Animal Care of The Ohio State University. Male Fischer rats were purchased from Taconic Farms (Germantown, NY) and were used for in vivo studies when they were 8–10 weeks old. Rats were anesthetized by intraperitoneal injection with ketamine (62.5 mg/kg of body weight) and xylazine (12.5 mg/kg of body weight) and positioned in a stereotactic apparatus. For tumor implantation, D74/HveC cells (2×10^5 cells in 2-μL Hanks' balanced salt solution [HBSS]) were implanted through a burr hole drilled in the skull at 3 mm lateral from the bregma and to a depth of 4 mm, as previously described (17). All rats in this tumor model form tumors and, if untreated, die by day 14 of tumor burden (17).

On day 5 after tumor cell implantation, the rats were randomly assigned to two groups; one group received an intraperitoneal injection of cyclophosphamide (CPA) (Bristol-Myers Squibb,

Princeton, NJ) at a dose of 80 mg/kg of body weight, and the other group received an equal volume of PBS. On day 7 after tumor cell implantation, anesthetized rats from each treatment group were randomly assigned to two groups; one group was treated with 1×10^7 plaque-forming units (pfu) of hrR3, and the other group received an equal volume (5 μL) of PBS, in both cases by direct intratumoral injection through the same burr hole that was used to implant the tumor cells. For studies involving cyclic Arg-Gly-Asp (cRGD) peptide, on day 3 after tumor cell implantation, the rats were randomly assigned to receive a direct intratumoral injection of 30 μg of cRGD peptide in 3 μL of PBS (EMD121974; Merck KGaA, Darmstadt, Germany) or 3 μL of PBS. On day 7 after tumor cell implantation, anesthetized rats from cRGD peptide– and PBS-treated groups were randomly assigned to receive 1×10^7 pfu of hrR3 or an equal volume (5 μL) of PBS by direct intratumoral injection. To investigate the effect of oncolytic virus treatment on blood vessels in rats, some rats (n = 6 rats per group) were treated with PBS or cyclophosphamide (day 5), or cRGD peptide (day 3) and then treated with PBS or oncolytic virus on day 7 after tumor implantation. Three days after oncolytic virus treatment, these rats were injected via the tail vein with 0.5 mL of 1 mg/mL Texas red–conjugated tomato lectin (Vector Laboratories Burlingame, CA) or 0.25 mL of 1 mg/mL fluorescein isothiocyanate (FITC)–conjugated dextran (>70 kDa; Sigma-Aldrich). Rats were killed by decapitation 5 minutes after injection of these compounds, and their brains were harvested and analyzed by fluorescence microscopy.

We also evaluated the effect of the doubly mutated rHSVQ oncolytic virus on tumor vasculature in a mouse glioma model. Female athymic nude mice (6–8 weeks old; National Cancer Institute, Bethesda, MD) were anesthetized by intraperitoneal injection with ketamine (50 mg/kg of body weight) and xylazine (25 mg/kg of body weight) and positioned in a stereotactic apparatus for tumor implantation. Human glioma U87ΔEGFR cells (1×10^5 cells in 4-μL HBSS) were implanted through a burr hole drilled in the skull at 2 mm lateral from the bregma and to a depth of 3 mm as previously described (19). Ten days after U87ΔEGFR cell implantation, mice (n = 6 mice per group) were randomly assigned to receive rHSVQ (1×10^5 pfu) or an equal volume (3 μL) of PBS by direct intracerebral injection through the same burr hole used for tumor cell injection. On day 3 after virus or PBS injection, the mice were injected with rhodamine conjugated to dextran (>70 kDa; Sigma-Aldrich) and killed by cervical dislocation 5 minutes later.

For survival studies, an additional 26 rats (n = 6 rats per group for PBS and OV treatment groups and n = 7 rats per group for cRGD and OV + cRGD treatment groups) were killed by decapitation when they became moribund, lethargic, anorexic, dehydrated, or distressed. The presence of intracranial tumors was macroscopically confirmed post mortem in all animals. To examine the effect of oncolytic virus on immune cell infiltration, an additional 16 rats (n = 4 rats per group for PBS, OV, CPA + OV, and cRGD + OV treatment groups) were killed on day 10 after tumor implantation (3 days after PBS or OV treatment) and tumor sections from harvested brains were evaluated by immunohistochemistry. To examine the effect of cRGD peptide treatment on OV induced inflammation, an additional nine rats (n = 3 rats per group for PBS, OV, and cRGD + OV treatment groups) were killed on day 10 after tumor implantation (3 days after PBS or OV treatment) and their tumor tissue was analyzed for expression of genes encoding inflammatory cytokines, chemokines, and their receptors. To analyze changes in interferon gamma (IFN-γ) protein levels in tumor tissue, an additional 16 rats (n = 4 rats per group for PBS, OV, CPA + OV, and cRGD + OV treatment groups) were killed by decapitation on day 10 after tumor implantation and tumor tissue lysate was analyzed by ELISA for Interferon-gamma expression by enzyme-linked immunosorbent assay (see below).

Brain Immunohistochemistry and Immunofluorescence

Animal brains from rats and mice were fixed in 4% paraformaldehyde, dehydrated in 30% sucrose and then frozen in an isopropanol–dry ice bath. Cryostat sections (10-μm thick) of frozen brains were thawed, rehydrated in PBS, and incubated with horse serum (Vector, Burlingame, CA) and hydrogen peroxide (30% solution, Sigma-Aldrich) to block nonspecific protein binding and endogenous peroxidase activity, respectively. Sections were incubated with one of the following primary antibodies: rabbit polyclonal anti-HSV1 capsid antibody (1:200 dilution; Abcam, Cambridge, MA); mouse monoclonal anti-rat CD45 antibody, which is specific for CD45-positive leukocytes (1:20 dilution; Serotec, Oxford, U.K.); or affinity-purified mouse monoclonal anti-rat CD31 antibody, which is specific for endothelial cells (1:10 dilution; Pharmingen, San Diego, CA). Biotin–conjugated horse anti-mouse or goat anti-rabbit immunoglobulin G antibody (both at 1:200 dilution; Vector) was used as the secondary antibody. The sections were washed and incubated for 30 minutes with Vectastain ABC reagent (Vector). The sections were washed extensively and incubated with the chromogen diaminobenzidine (DAKO, Carpinteria, CA). The sections were counterstained with hematoxylin, dehydrated with increasing concentrations of ethanol, and fixed in xylene. The area per view field (four view fields selected randomly from each tumor section [4 sections per tumor and 4 tumors per group]) was analyzed for the percentage of area staining positive for CD45 staining) positive for HSV- or CD45-staining was calculated with the use of ImageJ1.34n software (National Institutes of Health [NIH], Bethesda, MD).

For immunofluorescence staining, cryostat sections (20-μm thick) of frozen brain were thawed, rehydrated in PBS, and incubated overnight at 4 °C with one of the following primary antibodies diluted in PBS containing 1% bovine serum albumin and 0.1% Triton X-100: mouse anti-rat RECA-1 antigen, which recognizes rat endothelial cells (1:20 dilution; Serotec), or affinity-purified mouse monoclonal anti-rat CD31 antibody (1:20 dilution; Pharmingen). The sections were rinsed in PBS and incubated with Alexa Fluor 647–conjugated goat anti-mouse IgG1 (Molecular Probes, Eugene, OR) or FITC–conjugated donkey anti-mouse secondary antibody (Jackson Immuno Research, West Grove, PA) for 1 hour at room temperature. The sections were counterstained with 4′,6′diamidino-2-phenylindole hydrochloride and analyzed by fluorescence microscopy.

Microvessel Density

Microvessel density was analyzed in brain tumors from rats that had been injected 5 minutes before they were killed with FITC–dextran, which remains sequestered within blood vessels and thus highlights

functional perfused vessels. Brains from rats and mice were fixed in 4% paraformaldehyde, dehydrated in 30% sucrose, and then frozen in an isopropanol–dry ice bath. Cryostat sections (20-μm thick) of frozen brain were made. Tumor sections were scanned microscopically at low (×4) magnification to identify areas of highest vascularization (i.e., hot spots). Individual tumor microvessels in these hot spots were then counted under high magnification (×20), and the average vessel count in three hot spots was taken as the microvessel density per view field. Microvessel counting was performed in at least three sections per tumor and from four rats per group.

Virus Yield Assay

To evaluate effect of oncolytic virus on virus propagation in vivo, an additional 12 rats (n = 4 rats per group for PBS, OV, and cRGD + OV treatment groups) were killed 3 days after oncolytic virus treatment and the tumor-containing brain hemisphere was removed, weighed, placed in 2 mL of DMEM, homogenized by 50 passages through a syringe equipped with a 19-gauge needle, and subjected to three freeze–thaw cycles. After the final thaw, the cellular debris was pelleted by centrifugation (700g) and the virus-containing supernatants were collected and used for virus titration on Vero cells, as previously described (17).

Gene Expression Analysis

Total RNA was extracted from the brain tumor tissue of rats that had been treated with PBS or with oncolytic virus, either alone or following cRGD peptide pretreatment, with the use of TRIZOL reagent (Invitrogen, Carlsbad, CA), according to the manufacturer's instructions. Total RNA (4 μg) was converted to complementary DNA (cDNA) with the use of a SuperScript First-Strand cDNA Synthesis System (Invitrogen), according to the manufacturer's instructions. The cDNAs were then used for quantitative real-time polymerase chain reaction (PCR) analysis of gene expression, which was performed with the use of a model 7500 real-time PCR system (Applied Biosystems, Foster, CA). Each PCR assay was performed in a volume of 25 μL that contained 1 μM of each primer, 12.5 μL of 2 × SYBR Green Master Mix (Applied Biosystems), and 5 μL of a 1:100 dilution of cDNA. Each gene was amplified in triplicate. β-actin was used as an internal control. Primers for gene amplification, which were designed with the use of the Primer Express program (Applied Biosystems), were as follows: vascular endothelial growth factor (VEGF), forward, 5′-AAATCCTGGAGCGTTCACTGTG-3′, reverse, 5′-TAACTCAAGCTGCCTCGCCTT-3′; lacZ, forward, 5′-AATGGCTTTCGCTACCTGGA-3′, reverse, 5′-CCATCGCGTGGGCGTA-3′; and β-actin, forward, 5′-CTACAGATCATGTTTGAGACCTTCAAC-3′, reverse, 5′-CCAGAGGCATACAGGGACAAC-3′. Relative quantification of gene expression was calculated as 2d*Ct* test gene/2d*Ct* actin, where *Ct* is the number of cycles for saturation and d*Ct* is the difference in the number cycles needed for expression of a gene in a tumor from untreated rats (used as baseline) and the number of cycles needed for expression from rats receiving treatment (tumor alone or tumor plus oncolytic virus). The fidelity of all PCR assays was confirmed by agarose gel electrophoresis.

We used a Rat Inflammatory Cytokines & Receptors RT^2 Profiler PCR Array (Super Array Bioscience Corporation, Frederick, MD), according to the manufacturer's instructions, to evaluate changes in the expression of genes encoding 84 rat cytokines and their receptors in brain tumor tissue in response to oncolytic virus treatment (alone or in combination with cRGD) relative to expression in control (HBSS-treated) rats. The array includes controls to assess cDNA quality and DNA contamination. Volcano plot analysis (20) was used to compare the fold change in gene expression between groups to the level of statistical significance.

Magnetic Resonance Imaging

Magnetic resonance imaging (MRI) was acquired using an 8.0 Tesla MRI system (Magnex-GE, Abingdon, U.K.) equipped with a Bruker AVANCE console (Bruker, Billerica, MA) interfaced with Techron (Crown International, Elkhart, IN) gradient amplifiers and Magnex gradients (Magnex Scientific, Abingdon, U.K.) and a custom-built radiofrequency front end. A custom-made 3-cm diameter birdcage coil was tuned to the head of each rat at 340 MHz while the rat was anesthetized and placed in the prone position. A T_2*-weighted two-dimensional gradient echo (GRE) sequence and a T_2-weighted two-dimensional rapid acquisition with relaxation enhancement (RARE) sequence 3 days after implantation of oncolytic virus. Parameters for the GRE sequence were as follows: repetition time/echo time = 600/14.6 msec, flip angle = 45°, matrix = 512 × 512, field of view = 4 × 4 cm, acquisition time = 10 minutes 34 seconds, in-plane resolution = 78 μm. Parameters for the RARE sequence were as follows: repetition time/echo time = 5000/21.5 msec, flip angle = 90°, matrix = 256 × 256, field of view = 4 × 4 cm, acquisition time = 5 minutes 19 seconds, in-plane resolution = 156 μm. After the precontrast images were acquired, sequential GRE images were acquired at 0, 15, and 30 minutes following intravenous administration of the contrast agent ultra-small-particle iron oxide SHU 555 C (Supravist, Schering AG, Germany) at a dosage of 2 mg Fe/kg of body weight.

The signal intensity of regions of tumor was measured at each time point using Medical Imaging Processing, Analysis & Visualization (MIPAV) software (version 2.7; NIH). Subtracted images (precontrast image from each postcontrast image) were derived using an interactive data language–based program. To evaluate the USPIO leakage, temporal changes in signal intensity on both tumor region and contralateral hemisphere were calculated, and the percent of signal intensity was represented as the percent intensity relative to the intensity on the contralateral normal hemisphere in each section.

Interferon-Gamma Enzyme-Linked Immunosorbent Assay

Brain tumor samples from tumor-bearing rats (n = 4 rats per group) treated with PBS, oncolytic virus, cyclophosphamide and oncolytic virus, or cRGD peptide and oncolytic virus were suspended separately in an equal weight of radioimmunoprecipitation assay buffer (150 mM NaCl, 1% Nonidet P-40, 0.5% sodium deoxycholate, 0.1% sodium dodecyl sulfate, 150 mM Tris–HCl [pH 8.0]) and homogenized by 50 passages through a syringe equipped with a 19-gauge needle. The homogenate was centrifuged (10 000g) for 10 minutes at 4 °C, and the resulting supernatant was collected and used to quantify the concentration of IFN-γ with the use of an IFN-γ ELISA kit (R&D Systems, Inc., Minneapolis, MN).

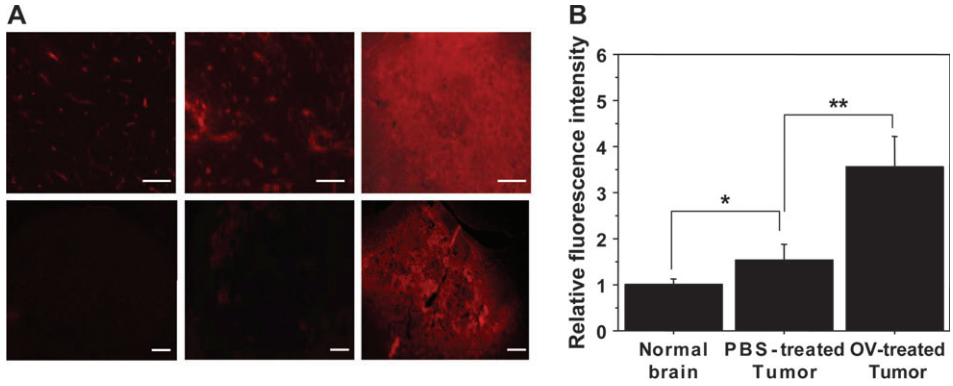

Fig. 1. Effect of oncolytic virus (OV) infection of rat intracerebral tumors on vascular permeability. Seven days after D74/HveC glioma cell implantation, rats with intracerebral brain tumors were treated with OV or phosphate-buffered saline (PBS) as a control by direct intracerebral injection. Three days after OV or PBS treatment, the rats were injected with Texas red–conjugated tomato lectin via the tail vein 5 minutes before they were killed (n = 6 rats per group). The brains were harvested and analyzed by immunofluorescence microscopy for changes in the tumor vasculature. **A**) Immunofluorescence images of brain vasculature. Shown are representative images of contralateral normal brain (left panels) and tumor area from control-treated (middle panels) and OV-treated (right panels) rats at ×20 (top row) and ×4 (bottom row) magnification. **Bar** = 50 μm (top panel) or 200 μm (bottom panel). **B**) Quantification of the leaked fluorescent dye in normal brain, PBS-treated tumor tissue, and OV-infected tumor tissue relative to the level in contralateral normal untreated brain in each slice. Data shown are the mean values and upper 95% confidence intervals of the intensity levels from four sections per rat and six rats per group. **P* = .029, ***P*<.001 (one-way analysis of variance followed by Scheffe's post hoc test, two-sided).

Statistical Analysis

Student's *t* test was used to test for the statistical significance of the percent loss in signal intensity in the MRI study and of the fold change in gene expression with quantitative PCR in the volcano plot analysis. One-way analysis of variance followed by Scheffe's post hoc test was used to compare relative fluorescent units, infectious viral titers, areas of CD45-positive infiltrating leukocytes, and oncolytic virus–encoded LacZ gene expression. Kaplan–Meier curves were compared using the log-rank test. A *P* value less than .05 was considered to be statistically significant in Student's *t* test and Scheffe's test. All statistical tests were two-sided. All statistical analyses were performed with the use of SPSS statistical software (version 14.0; SPSS, Inc., Chicago, IL).

Results

Vascular Permeability in Oncolytic Virus–Treated Brain Tumors

We first confirmed that Texas red–conjugated lectin and FITC–conjugated dextran injected intravenously into rats shortly before killing could be used to visualize vasculature of brain tumors in rats that received intracranial injection with glioma cells. These compounds were injected into the tail veins of rats (n = 3 rats per group) that had been implanted 7 days earlier with D74/HveC glioma cells immediately before they were killed to visualize vasculature of brain tumors. Fluorescence microscopy of sections of normal untreated brain that were stained with anti-CD31 antibody to detect endothelial cells confirmed that both Texas red–conjugated lectin and FITC–conjugated dextran were sequestered within blood vessels in the normal untreated rat brain (Supplementary Fig.1, available online).

To examine the physiologic changes induced in the tumor vasculature by oncolytic virus treatment, we employed a syngeneic immunocompetent rat glioma model of brain tumors. Seven days after intracerebral D74/HveC glioma cell implantation, the resulting rat brain tumors were treated with hrR3 or PBS by direct intracerebral injection. Sections of brain tumors that were harvested from rats 3 days after treatment with hrR3 or PBS (i.e., 10 days after tumor cell implantation) were examined by fluorescence microscopy (n = 6 rats per group) for the fluorescent dye injected by tail vein 5 minutes before killing. In the contralateral (i.e., untreated normal brain) hemisphere of all rats, the injected fluorescent dye remained sequestered within blood vessels (Texas red–lectin, Fig. 1; FITC–dextran, Supplementary Fig. 2, available online). The relative fluorescence units (RFU) for each section were determined by comparing the fluorescence intensity of the tumor area with the fluorescence intensity of the corresponding contralateral normal untreated brain in each section (Fig. 1; Supplementary Fig. 2, available online). The normal brain sections revealed the presence of an intact blood–brain barrier in all rats. Sections of tumor area from PBS-treated tumor-bearing rats revealed the presence of a tortuous and leaky tumor vasculature, resulting in a higher fluorescence relative to normal brain. Sections of brain tumors after direct oncolytic virus infection revealed a further increase in the vascular leakage of the oncolytic virus–treated tumors, as evidenced by the higher mean fluorescence compared with that in the contralateral normal hemisphere. Quantification of RFU in brain sections revealed that oncolytic virus–treated tumor sections had statistically significantly higher mean RFU than PBS-treated tumor sections, indicating that oncolytic virus treatment increased vascular permeability (oncolytic virus tumor versus PBS tumor, mean RFU = 3.56 versus 1.53, difference = 2.02, 95% confidence interval [CI] = 1.53 to 2.51, *P*<.001) (Fig. 1, B).

We further confirmed the generality of the vascular hyperpermeability observed after oncolytic virus treatment of brain tumors in an athymic nude mouse model of brain tumors using a different oncolytic virus (HSVQ) (Supplementary Fig. 3, available online). In all cases, increased vascular leakage was observed in tumors that were treated with oncolytic virus compared with that in PBS-treated control tumors.

Further confirmation of the increased capillary permeability of glioma blood vessels in rats treated with oncolytic virus compared with PBS was derived from 8.0 Tesla high-resolution GRE MRIs acquired 3 days after treatment. Sequential subtractions of images obtained before contrast from those obtained 0–30 minutes after contrast revealed prolonged signal loss within the microvascular bed of oncolytic virus–treated tumors compared with PBS-treated

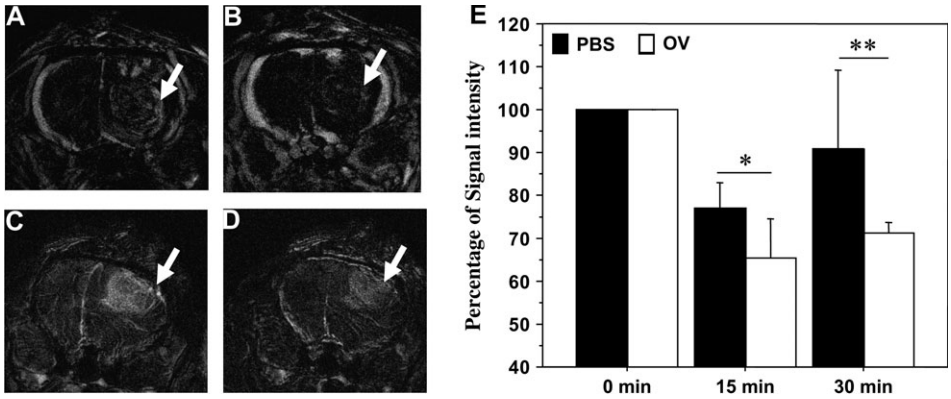

Fig. 2. Magnetic resonance imaging of tumor vasculature in live rats before and after injection of ultra-small particles of iron oxide (USPIO). Three days after oncolytic virus (OV) or phosphate-buffered saline (PBS) treatment, rats (n = 3 per group) were scanned on an ultra high-field high-resolution 8.0-T magnetic resonance imager using a T_{2*}-weighted gradient echo sequence before and after USPIO was administrated through a femoral vein catheter. Subtracted images (after USPIO minus before USPIO) of a tumor from a PBS-treated rat (**A**) 15 minutes and (**B**) 30 minutes after USPIO administration. Subtracted images (after USPIO minus before USPIO) of a tumor from an OV-treated rat (**C**) 15 minutes and (**D**) 30 minutes after USPIO administration. **E**) Quantification of percent loss in signal intensity compared with the contralateral normal hemisphere in OV-treated rats at the indicated times after USPIO administration. Data shown are mean values of the intensity levels for three rats; error bars correspond to 95% confidence intervals. **P* = .037, ***P* = .04 (two-sided Student's *t* test).

tumors, reflecting increased vascular permeability (Fig. 2). Quantification of percent loss in signal intensity compared with contralateral normal hemisphere in oncolytic virus–treated rats at the indicated times after USPIO administration revealed a statistically significant increase in vascular hyperpermeability at both 15 minutes (PBS versus oncolytic virus treatment: mean percentage of signal intensity relative to contralateral normal brain = 77% versus 65%, difference = 12%, 95% CI = 1% to 22%; *P* = .037) and 30 minutes (PBS versus oncolytic virus treatment: mean percent of signal intensity relative to contralateral normal hemisphere = 91% versus 71%, difference = 20%, 95% CI = 2% to 37%; *P* = .04) after oncolytic virus treatment relative to PBS-injected rats. Taken in conjunction with the leakage of the fluorescent dye observed by immunofluorescence microscopy, these results demonstrate the increased permeability of the tumor vasculature of oncolytic virus–treated glioma.

Effect of Oncolytic Virus Treatment on Inflammation

Oncolytic virus treatment of brain tumors can evoke a rapid innate immune response that increases immune cell infiltration into the tumors (17,21). Vasodilation and hyperpermeability are the earliest physiologic responses to viral infection and, as such, are characteristics of a physiologic inflammatory response to a viral infection (21,22). To investigate whether the increase in the observed vascular leakage in oncolytic virus–treated rats was associated with tumor tissue inflammation, we used quantitative real-time PCR and gene expression array analysis of tumor tissue harvested 3 days after oncolytic virus or PBS treatment to examine changes in expression of genes known to induce inflammation (n = 3 rats per group). Fig. 3, A, shows a volcano plot of the fold change in the expression of 84 genes encoding inflammatory cytokines and their receptors for oncolytic virus–treated tumor tissue compared with PBS-treated tumor tissue versus the level of statistical significance of the change. Oncolytic virus treatment induced at least a twofold increase or decrease in the expression of 50 genes relative to expression in the PBS-treated tumors (Supplementary Table 1, available online). Of these 50 genes, 48 displayed an increase in expression in the oncolytic virus–treated tumors compared with the control-treated tumors, suggesting that oncolytic virus treatment induced an inflammatory response. This increase in inflammatory cytokine

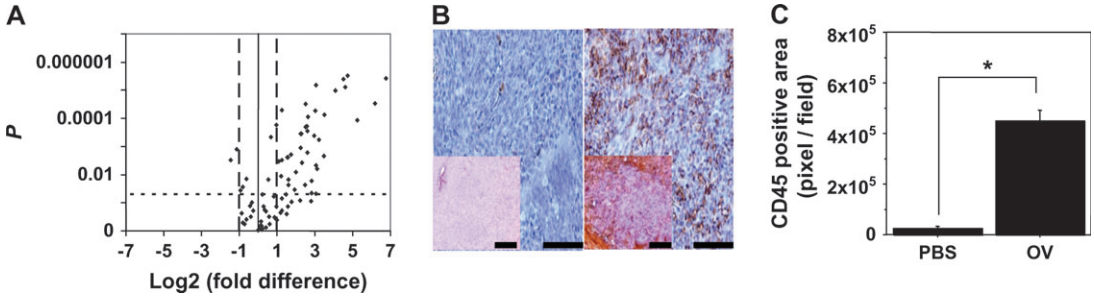

Fig. 3. Oncolytic virus (OV)–induced inflammation. Three days after OV or phosphate-buffered saline (PBS) treatment, rats were killed and their tumor tissue was analyzed for gene expression by quantitative real-time polymerase chain reaction analysis or subjected to immunohistochemistry (n = 3 rats per group). **A**) Volcano plot of OV-induced changes in expression of genes for 84 inflammatory cytokines and their receptors. This plot arranges genes along dimensions of biologic and statistical significance. The *x*-axis indicates the $\log_2$ fold difference in gene expression for OV-treated versus control PBS–treated tumor tissue, and the *y*-axis indicates *P* values obtained from the gene-specific *t* test on a negative log scale. The **solid black vertical line** indicates no change relative to control, and **dashed vertical lines** indicate a twofold change in OV-treated samples relative to control. The **horizontal dotted blue line** indicates the threshold for a *P* value of .05 for the *t* test. Each **point** represents the mean value of the change in expression of an individual chemokine or chemokines receptor gene in OV-treated tumors relative to control PBS–treated tumors. **B**) Immunohistochemistry for CD45-positive infiltrating leukocytes in rat brain tumors 3 days after OV infection. Infiltrating CD45-positive cells (**brown**) in OV-infected tumor sections (right panel) and control PBS–treated tissue (left panel) at ×20 magnification. Insets show low magnification (×4) images of the respective PBS- and OV-treated tumor sections. **Bar** = 50 μm (×20 images) or 100 μm (×4x images). **C**) Quantification of CD45-positive leukocyte infiltration in tumor tissue in response to OV infection. Data shown are the mean values and upper 95% confidence intervals of CD45-positive staining area per view field for four sections per rat for four rats per group. **P*<.001 (two-sided Student's *t* test).

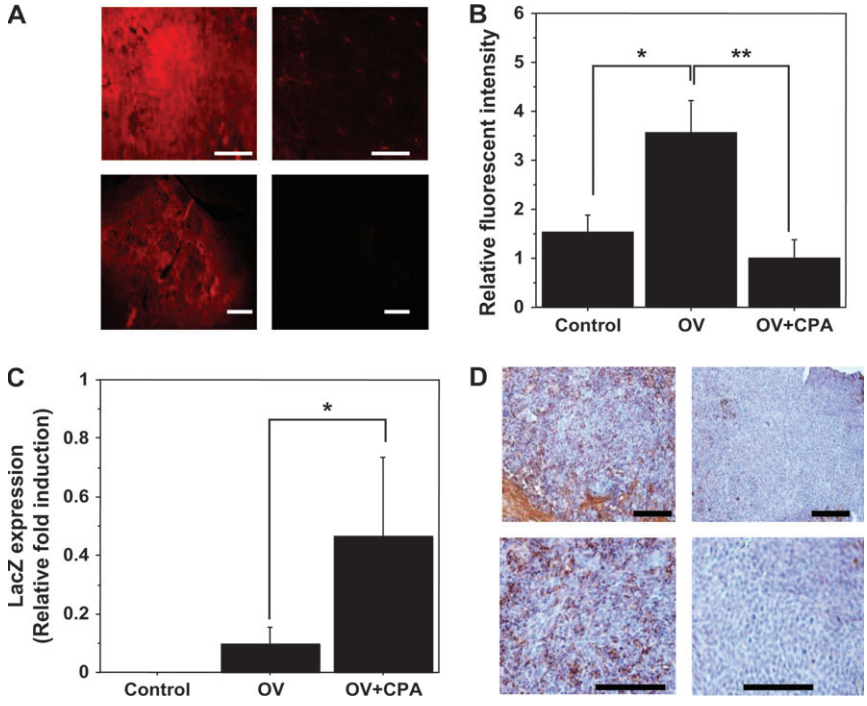

Fig. 4. Effect of cyclophosphamide (CPA) on oncolytic virus (OV)–induced changes in the tumor microenvironment. Rats bearing intracerebral brain tumors were treated with CPA or phosphate-buffered saline (PBS) by intraperitoneal injection on day 5 after glioma cell implantation, followed on day 7 by intracranial injection with OV or PBS. Three days later, the rats were injected via the tail vein with Texas red–conjugated lectin and were killed 5 minutes later (n = 6 rats per group). Brains and tumors were harvested and analyzed. **A**) Fluorescence microscopy of Texas red-lectin–perfused tumor vasculature. Shown are images of tumors derived from rats treated with OV (left panels) and with OV after CPA pretreatment (right panels) at ×20 (top row) and ×4 (bottom row) magnification. **Bars** = 50 μm in ×20 images and 200 μm in ×4 images. **B**) Quantification of the leaked fluorescent dye relative to that in the contralateral normal brain in each section for tumor treated with PBS or OV and for tumors treated with CPA before OV treatment. Data shown are the mean values and upper 95% confidence intervals of the intensity levels from four sections per rat of six rats per group **P*<.001, ***P*<.001 (one-way analysis of variance followed by Scheffe's post hoc test, two-sided). **C**) Quantitative real-time polymerase chain reaction analysis of OV–encoded LacZ gene expression in tumors treated with PBS or OV and in tumors treated with CPA before OV treatment. Data shown are the mean values and upper 95% confidence intervals of the relative expression of the LacZ gene to the β-actin gene for four rats per group. **P* = .007 (one-way analysis of variance followed by Scheffe's post hoc test, two-sided). **D**) Immunohistochemistry for CD45–positive infiltrating leukocytes (**brown**) in brain tumors from rats pretreated with PBS (left panels) or CPA (right panels) at ×10 (top row) and ×20 (bottom row) magnification. **Bars** = 50 μm.

gene expression was accompanied by a substantial increase in infiltration of CD45-positive leukocytes into intracerebral tumors after oncolytic virus treatment (Fig. 3, B). Quantification of the CD45-positive staining area per field of view revealed a statistically significant increase in the infiltration of CD45-positive leukocytes in tumor tissue treated with oncolytic virus relative to PBS-treated tumor tissue (oncolytic virus–treated versus PBS-treated tumor, mean = 4.5×10^5 pixels per field versus 2.3×10^4 pixels per field, difference = 4.2×10^5 pixels per field, 95% CI = 3.5×10^5 to 5.0×10^5 pixels per field; *P*<.001) (Fig. 3, C). Together, these results suggest that a local inflammatory response was activated in the oncolytic virus–treated tumors. We observed no change in the expression of the gene encoding VEGF, a potent vascular permeability factor, in oncolytic virus–treated tumor tissue (data not shown).

To confirm the role of the immune response in oncolytic virus–induced vascular hyperpermeability, we evaluated changes in oncolytic virus–induced vascular leakage in tumor-bearing rats that had been treated with cyclophosphamide before oncolytic virus injection. In addition to its immunosuppressive effects, cyclophosphamide blocks inflammation and reduces viral clearance, both of which increase the propagation of oncolytic viruses, thereby enhancing therapeutic efficacy of oncolytic viruses (11,12,17,23–25). Tumor-bearing rats treated with cyclophosphamide or PBS on day 5 after tumor cell implantation were treated with oncolytic virus on day 7 and then killed on day 10, five minutes after tail vein injection of Texas red–lectin (Fig. 4, A) or FITC–conjugated dextran (Supplementary Fig. 3, available online), and sections of their brain were examined by fluorescence microscopy (n = 6 rats per group). There was a substantial decrease in the amount of leaked fluorescent dye in tumor sections from oncolytic virus–treated rats pretreated with cyclophosphamide compared with control PBS-treated rats (Fig. 4, A; Supplementary Fig. 3, A–C, available online). Quantification of the leaked Texas red–lectin revealed statistically significant reduction in fluorescence in tumor sections from rats pretreated with cyclophosphamide than in rats not pretreated (mean RFU = 3.56 versus 0.99, respectively; difference = 2.56, 95% CI = 2.07 to 3.06; *P*<.001) (Fig. 4, B). These results indicate that cyclophosphamide pretreatment suppressed oncolytic virus–induced vascular leakage in tumor tissue of rats.

We further investigated the effect of cyclophosphamide treatment on the propagation of oncolytic virus in tumors and on CD45–positive leukocyte infiltration in tumor tissue. On day 5 after glioma cell implantation, rats were pretreated with PBS or cyclophosphamide, and, on day 7, they were treated with oncolytic virus or PBS. The rats were killed 3 days after oncolytic virus treatment and their brain tumors were analyzed for expression of the oncolytic virus–encoded gene for β-galactosidase. PBS-treated tumors were used as a negative control. Quantitative real-time PCR revealed a statistically significant 5.1-fold increase (95% CI = 1.6- to 6.7-fold, *P* = .007) in oncolytic virus–encoded β-galactosidase gene expression in cyclophosphamide-pretreated tumors compared with PBS-pretreated tumors (Fig. 4, C). Moreover, leukocyte infiltration was much lower in tumors pretreated with cyclophosphamide before oncolytic viral therapy than in tumors pretreated with PBS (Fig. 4, D), which is consistent with published findings (11). In addition, cyclophosphamide pretreatment did not affect the percentage of endothelial cells that stained positive for HSV (Supplementary Fig. 3, D, available online). Collectively, these data indicate that cyclophosphamide suppressed oncolytic virus–induced changes in vascular permeability of tumors.

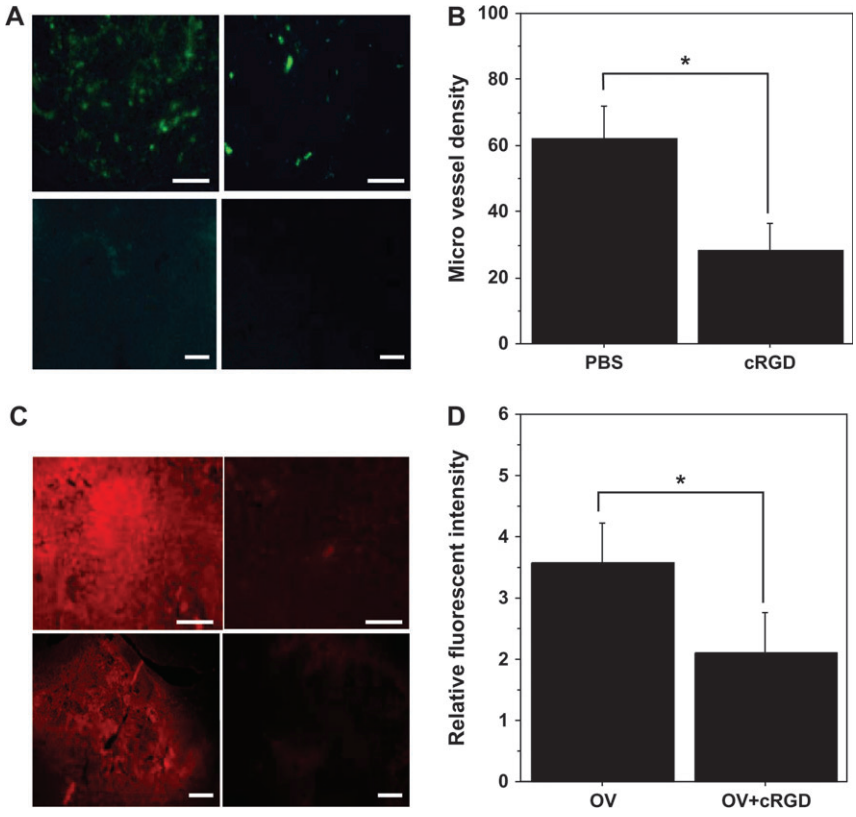

Fig. 5. Effect of cRGD peptide treatment on angiogenesis in rat glioma. Rats bearing brain tumors were treated with 30 μg of cRGD peptide or with phosphate-buffered saline (PBS) 3 days after intracerebral glioma cell implantation. Rats were injected with fluorescein isothiocyanate (FITC)–conjugated dextran via the tail vein 5 minutes before they were killed on day 10 after glioma cell injection (i.e., 7 days after cRGD or PBS pretreatment). Brains were harvested and sectioned for analysis. **A**) Fluorescence microscopy of FITC-dextran–perfused tumor blood vessels. Shown are representative images of tumors derived from rats treated with PBS (left panels) or cRGD (right panels) at ×20 (top row) and ×4 (bottom row) magnification. **Bars** = 50 μm in ×20 images and 200 μm in ×4 images. **B**) Quantification of tumor microvessel density. Data shown are the mean tumor microvessel density defined as the number of blood vessels per view field and upper 95% confidence intervals from four sections per rat for four rats per group. *P = .009 (two-sided Student's t test). Rats with brain tumors were treated with cRGD or PBS on day 3 after glioma cell implantation and then with oncolytic virus (OV) on day 7. Rats were injected with Texas red–conjugated lectin via the tail vein 5 minutes before they were killed on day 10, (i.e., 7 days after cRGD or PBS treatment) and their brains were harvested and sectioned and tumor-bearing brain sections were analyzed by fluorescent microscopy for the effect of cRGD treatment on OV-induced vascular leakage (n = 4 rats per group). **C**) Fluorescence microscopic images of rat brain sections from OV-infected rats pretreated with PBS (left panels) or cRGD peptide (right panels) at ×20 (top row) and ×4 (bottom row) magnification. **Bars** = 50 μm in ×20 images and 200 μm in ×4 images. **D**) Quantification of the intensity of the fluorescent dye relative to the contralateral normal brain in each section in OV-treated tumors from rats pretreated with cRGD or PBS. Data shown are the mean values and upper 95% confidence intervals of the fluorescence intensity levels from four sections per rat for four rats per group. *P = .02 (two-sided Student's t test).

Effect of cRGD Treatment on Tumor Angiogenesis

Increased vascularity has been associated with increased tissue edema, cellular infiltrates, and the induction of an inflammatory response (22,26). Conversely, reduction in the number of blood vessels is associated with reduced tissue inflammation (27). These observations have led to the idea of targeting angiogenesis to reduce inflammation (28,29). We hypothesized that treatment of tumor-bearing rats with cRGD peptide, which is a potent inhibitor of angiogenesis and glioma growth in vivo (13,30), before oncolytic virus therapy should reduce oncolytic virus–induced vascular leakage and tumor infiltration by immune cells and improve the efficacy of oncolytic virus treatment. On day 3 after tumor cell implantation, rats were treated with cRGD or PBS (n = 4 rats per group), and, on day 10, the rats were injected with FITC–dextran 5 minutes before euthanasia. Their tumors were harvested, sectioned, and analyzed to examine the effect of cRGD on tumor microvessel density (Fig. 5, A and B). Tumors from rats treated with cRGD had statistically significantly lower microvessel density than tumors from control rats treated with PBS, confirming the antiangiogenic effect of cRGD peptide in rat glioma (mean microvessel density for cRGD versus PBS = 62.2 versus 27.9 blood vessels per view field, difference = 34.3 blood vessels per view field, 95% CI = 13.9 to 54.8 blood vessels per view field, P = .009). The statistically significant decrease in the number of perfused functional vessels per view field was also accompanied by a substantial reduction in the number of tumor blood vessels, as visualized by immunostaining with an anti-CD31 antibody specific for endothelial cells (Supplementary Fig. 4, available online).

Effect of cRGD Treatment on Oncolytic Virus–Induced Vascular Permeability and Immune Cell Infiltration

We next compared the effect of pretreatment with cRGD peptide on vascular permeability and immune cell infiltration in tumors of rats that were subjected to oncolytic virus treatment. Three days after tumor cell implantation, rats were treated with PBS or cRGD peptide. Four days later, they were treated with oncolytic virus. Three days after oncolytic virus injection, the rats were injected with Texas red–conjugated lectin, killed, and their tumors were sectioned and analyzed by fluorescence microscopy and immunohistochemistry for endothelial cell marker CD31. Immunohistochemistry for endothelial cell marker CD31 revealed a substantial reduction in the number of blood vessels in tumor sections from rats pretreated with cRGD before oncolytic virus injection compared with tumor sections from rats pretreated with PBS before oncolytic virus injection (Supplementary Fig. 5, B, available online). Fluorescence microscopy of tumor sections revealed that rats pretreated with cRGD peptide had substantially less vascular leakage of Texas red–lectin than rats pretreated with PBS (n = 4 rats per group) (Fig. 5, C). Quantification of the relative fluorescence intensity revealed statistically significantly lower mean fluorescence in tumor sections obtained from rats pretreated with cRGD compared with rats pretreated with PBS before oncolytic virus

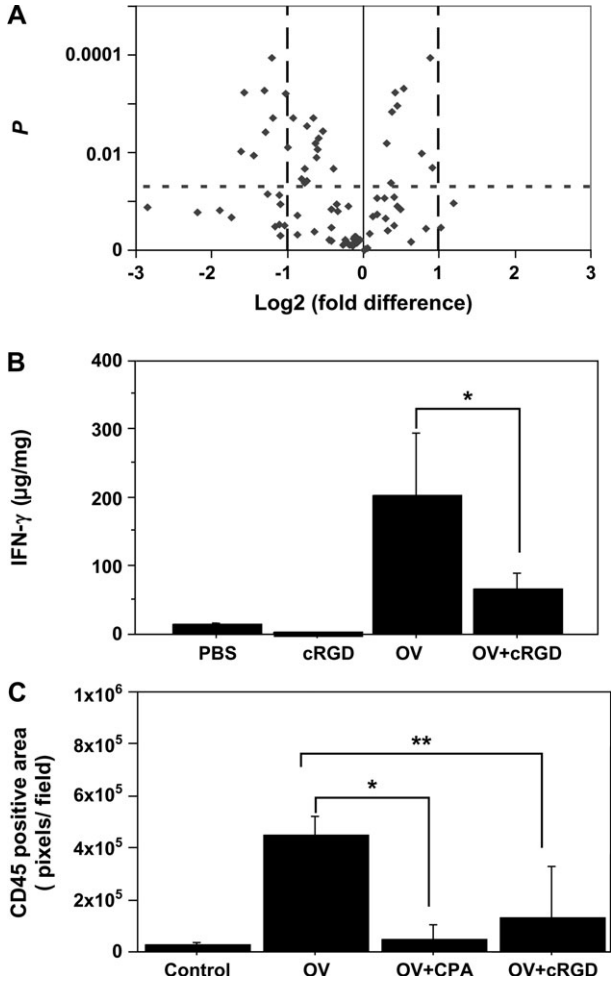

Fig. 6. Effect of cRGD peptide on oncolytic virus (OV)–induced inflammation. **A**) Volcano plot of OV-induced change in the expression of genes for 84 inflammatory cytokines and their receptors in response to cRGD peptide pretreatment. This plot arranges genes along dimensions of biologic and statistical significance. The *x*-axis indicates the $\log_2$ fold difference in gene expression for OV-treated versus control phosphate-buffered saline (PBS)–treated tumor tissue, and the *y*-axis indicates *P* values obtained from the gene-specific *t* test on a negative log scale. The **solid black vertical line** indicates no change relative to control, and **dashed vertical lines** indicate a twofold change in OV-treated samples pretreated with cRGD compared with OV-treated samples pretreated with PBS. The **horizontal dotted line** indicates the threshold for a *P* value of .05 for the *t* test. Each data point represents the mean values of the change in expression of an individual chemokine or chemokine receptor gene in OV- and cRGD-treated tumors relative to OV-treated tumors (n = 3 rats per group). **B**) Interferon gamma (IFN-γ) protein levels in tumor tissue lysates as measured by a rat IFN-γ enzyme-linked immunosorbent assay. Data shown are the mean values of IFN-γ protein levels per mg of tumor tissue and upper 95% confidence intervals from four rats per group. **C**) Quantification of CD45-positive cell infiltration in tumor tissue. Rats with brain tumors were treated with PBS or OV (day 7 after tumor cell implantation) alone or in conjunction with CPA treatment (on day 5 after tumor cell implantation) or cRGD peptide pretreatment (day 3 after tumor cell implantation) before OV treatment. Data shown are the mean values and upper 95% confidence intervals of CD45 staining area per view field for four sections per rat for four rats per group. **P* = .007, and ***P* = .019 (one-way analysis of variance followed by Scheffe's post hoc test, two-sided).

treatment (mean RFU for PBS versus cRDG = 3.56 versus 2.09, difference = 1.46, 95% CI = 0.38 to 2.55, *P* = .020) (Fig. 5, D). Similar results were obtained for rats pretreated with cRGD or PBS and injected with FITC–conjugated dextran (>70 kDa) immediately before they were killed (Supplementary Fig. 5, A, available online).

We next tested the effect of cRGD peptide on oncolytic virus–induced inflammation by examining changes in the expression of genes encoding inflammatory cytokines and their receptors. Fig. 6, A, shows a volcano plot of the fold change in gene expression for oncolytic virus–treated tumor tissue in rats that were pretreated with cRGD peptide compared with PBS-pretreated rats versus the level of statistical significance of the change. Supplementary Table 2 (available online) lists the 21 genes whose expression increased or decreased by more than twofold in tumors pretreated with cRGD versus with PBS before oncolytic virus therapy. Expression of 19 of the 21 dysregulated genes was decreased in tumor tissue pretreated with cRGD peptide compared with PBS pretreatment, indicating that oncolytic virus–induced inflammatory responses were suppressed in rats pretreated with cRGD peptide. Notably, 16 of the 19 genes whose expression decreased upon cRGD pretreatment displayed increased expression in oncolytic virus–treated tumor tissue (Supplementary Table 2, available online). A similar analysis of cytokine gene expression in peripheral blood mononuclear cells from tumor-bearing rats revealed no substantial change in expression of the 84 genes encoding inflammatory cytokines or their receptors in rats pretreated with cRGD compared with rats pretreated with PBS before oncolytic virus therapy (data not shown). It is also notable that the expression of genes encoding IFN-γ and IFN-γ–induced proteins such as CXCL11 and CXCL9 was increased by oncolytic virus treatment and decreased by pretreatment with cRGD peptide (Supplementary Tables 1 and 2, available online). IFN-γ is a secreted chemokine known to play a key role in orchestrating host immune responses to viruses (31). We have previously shown (11) that the addition of exogenous IFN-γ to rat glioma cells is sufficient to inhibit oncolytic virus replication in vitro. We have also observed increased viral presence (as observed by increased oncolytic virus–encoded LacZ expression) in gliomas that are established in IFN-γ knockout mice than in wild-type mice in vivo (11). We further confirmed the change in IFN-γ gene expression by using an ELISA to examine IFN-γ protein levels in cRGD-pretreated tumors. Tumors from rats pretreated with cRGD peptide before oncolytic virus treatment had statistically significantly lower IFN-γ levels than tumors pretreated with PBS (mean IFN-γ level, cRGD pretreatment versus PBS pretreatment = 203 versus 65.6 μg/mg, difference = 137 μg/mg, 95% CI = 72.7 to 202.9 μg/mg, *P* = .006) (Fig. 6, B). Together, these results indicate that cRGD treatment of tumors before oncolytic virus therapy reduced the vascular permeability and the production of inflammatory cytokines induced by oncolytic virus treatment of gliomas.

We next compared the effect of cRGD pretreatment on recruitment of leukocytes into tumor tissue after oncolytic virus treatment with the effect of cyclophosphamide pretreatment. Rats were treated with either cyclophosphamide or PBS 5 days after tumor cell implantation by intraperitoneal injection. Another group of rats was treated with either cRGD peptide or PBS 3 days after tumor cell implantation by direct intracerebral injection. Seven days after tumor cell implantation each group of rats was randomly assigned to receive oncolytic virus or PBS. The animals were killed 3 days after oncolytic virus treatment (day 10 after tumor cell implantation), and

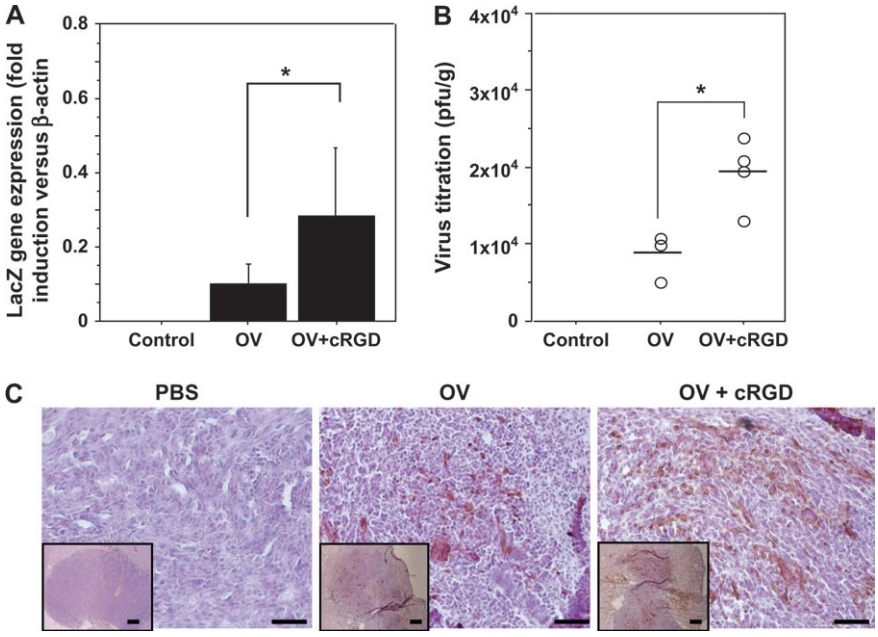

Fig. 7. Effect of cRGD peptide pretreatment on oncolytic virus (OV) replication in tumors. Rats with brain tumors were treated with phosphate-buffered saline (PBS) or cRGD peptide on day 3 after tumor cell implantation and then with PBS or OV on day 7 after tumor cell implantation. Rats were killed 3 days after OV infection of tumors (day 10 after tumor cell implantation), and their brains were harvested and analyzed for markers of oncolytic viral presence in tumors. **A**) Expression of OV-encoded LacZ gene measured by a quantitative real-time polymerase chain reaction assay. Data shown are the mean values of relative expression of the LacZ gene compared with that of the β-actin gene in each sample and upper 95% confidence intervals from 4 rats per group. **P* = .028 (one-way analysis of variance followed by Scheffe's post hoc test, two-sided). **B**) OV titration. Data points shown represent the values of infectious viral particles obtained per mg of tumor tissue samples from rats pretreated with cRGD peptide or PBS (n = 4 rats per group). **Horizontal bars** represent the mean value for each group. **P* = .0142 (one-way analysis of variance followed by Scheffe's post hoc test, two-sided). **C**) Immunohistochemical staining for herpes simplex virus (HSV) particles in rat brain tumors infected with OV, with or without cRGD pretreatment at ×20 magnification. Insets show representative low magnification images of the indicated tumor section stained for HSV. **Bars** = 50 μm in ×20 images and 200 μm in ×4 images.

tumor sections were analyzed by immunohistochemistry for CD45–positive leukocyte infiltration of tumor tissue (4 sections per rat, n = 4 rats per group) by immunohistochemistry.

Quantification of the CD45-stained area per view field revealed a statistically significant increase in infiltration of CD45–positive leukocytes in tumor tissue treated with oncolytic virus relative to PBS-treated tumor tissue (oncolytic virus–treated versus PBS-treated tumor, mean 4.48×10^5 versus 0.235×10^5 pixels per field, difference = 4.25×10^5 pixels per field, 95% CI = 3.53×10^5 to 4.96×10^5 pixels per field, $P<.001$). This increase in infiltrating leukocytes was suppressed in rats pretreated with cyclophosphamide before oncolytic virus therapy (mean CD45-positive area for oncolytic virus versus oncolytic virus + cyclophosphamide = 4.48×10^5 versus 0.47×10^5 pixels per field, difference = 4.01×10^5 pixels per field, 95% CI = 3.12×10^5 to 4.91×10^5 pixels per field; $P = .007$). There was also a statistically significant decrease in infiltrating leukocytes in tumors of animals pretreated with cRGD before oncolytic virus therapy compared with that in animals pretreated with PBS before oncolytic virus therapy (mean CD45-positive area for oncolytic virus versus oncolytic virus + cRGD peptide = 4.48×10^5 versus 1.30×10^5 pixels per field, difference = 3.18×10^5 pixels per field, 95% CI = 0.550×10^5 to 5.81×10^5 pixels per field, $P = .019$ (Fig. 6, C). There was no statistically significant difference in the level of suppression of OV-induced infiltrating leukocytes obtained by pretreatment with CPA (13-fold suppression for OV versus OV + CPA) and by pretreatment with cRGD (10.4-fold suppression for OV versus OV + cRGD) (OV + CPA versus OV + cRGD, $P = 0.7$).

Effect of cRGD Peptide on Oncolytic Virus Replication in Tumors

Next we tested the effect of pretreatment with cRGD peptide on oncolytic virus replication in tumors compared with pretreatment with PBS before oncolytic virus treatment. Rats were treated with cRGD peptide or PBS on day 3 after tumor cell implantation and with oncolytic virus or PBS on day 7 after tumor cell implantation. The rats were killed 3 days later, and tumor sections were analyzed for presence of oncolytic virus by quantitative real-time PCR for virus-encoded LacZ gene expression and for the amount of infectious viral particles obtained in each tumor, as measured by a standard plaque assay. Rats pretreated with cRGD peptide before oncolytic virus treatment had tumors with statistically significantly higher viral LacZ gene expression compared with rats treated with PBS before oncolytic virus treatment (mean fold increase in LacZ for OV + cRGD versus OV = 2.8-fold, 95% CI = 0.14- to 3.5-fold, $P = .028$) and statistically significantly higher titers of infectious virus (mean viral titer/mg tumor tissue for oncolytic virus + cRGD versus oncolytic virus = 1.93×10^4 pfu/mg versus 0.893×10^4 pfu/mg, difference = 1.04×10^4 pfu/mg, 95% CI = 3.46×10^3 to 1.73×10^4, $P = .0063$) (Fig. 7, A and B). Immunohistochemistry revealed that tumor tissue from cRGD peptide–pretreated rats had increased staining for HSV particles compared with that in tumor tissue from rats that were not pretreated (Fig. 7, C). These findings confirm that pretreatment with the antiangiogenic agent cRGD peptide increased the persistence of oncolytic viral in tumors.

Effect of cRGD Peptide Pretreatment on the Therapeutic Efficacy of Oncolytic Virus Treatment of Rat Gliomas

We next compared survival of oncolytic virus–treated rats that were pretreated with cRGD peptide with that of rats pretreated with PBS. Rats with brain tumors were pretreated with cRGD peptide or PBS on day 3 and then with PBS or oncolytic virus on day 7 after tumor cell implantation. The survival of rats in each group (n = 6 rats per group) was then compared by Kaplan–Meier analysis (Fig. 8). Control rats treated with PBS (on days 3 and 7) had a median survival of 13 days after tumor cell implantation, whereas rats treated with PBS on day 3 and with oncolytic virus on day 7 had

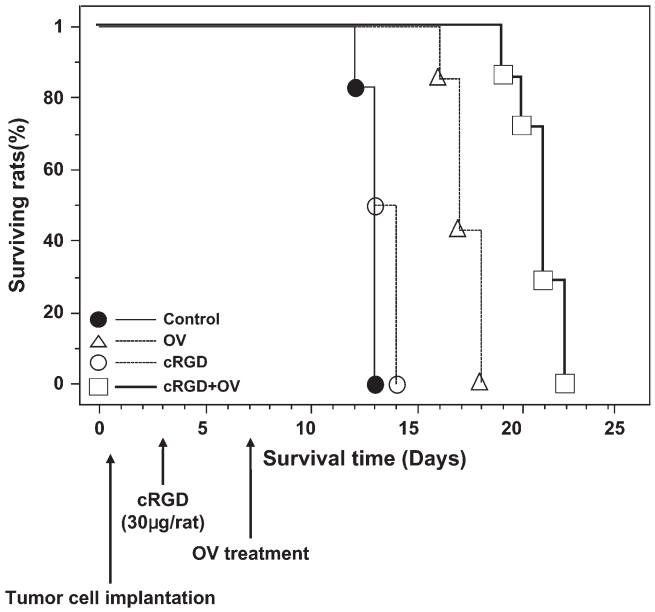

Fig. 8. Effect of cRGD peptide pretreatment on the therapeutic efficacy of oncolytic virus (OV) treatment of rat gliomas. Rats with brain tumors were pretreated with cRGD peptide or phosphate-buffered saline (PBS) 3 days after tumor cell implantation. Four days later, the rats were treated with OV or PBS. All rats were monitored closely and killed when they displayed signs of morbidity. Survival of animals in each group (control: PBS-only treated, cRGD: cRGD-only treated, OV: OV-only treated, and cRGD + OV: cRGD- and OV-treated rats) was analyzed by the log-rank test (n = 6 rats for the control and cRGD groups, n = 7 rats each for the OV and OV + cRGD groups).

a median survival of 17 days after tumor cell implantation. Rats treated with a single dose of cRGD peptide (cRGD on day 3 and PBS on day 7) had a median survival that was similar to that of PBS-treated rats (i.e., 13 days). However, rats that were pretreated with cRGD peptide (day 3) before oncolytic virus therapy (day 7) had statistically significantly longer median survival than rats treated with oncolytic virus alone (21 days versus 17 days, log-rank $P<.001$). Although the difference in survival was only a few days, it was an improvement of 23.5% over OV treatment and represents an improvement of 61.5% over PBS treatment in this very aggressive glioma model, in which PBS treated animals begin dying of tumor burden by day 13. This increase in the median survival of rats treated with cRGD and oncolytic virus compared with rats treated with PBS and oncolytic virus was observed only when cRGD peptide treatment was given before oncolytic virus injection; it was not observed when cRGD peptide was given at the same time as oncolytic virus (data not shown). These findings indicate that the cRGD peptide–mediated antiangiogenic effect improved the therapeutic efficacy of oncolytic virus treatment in this rat glioma model.

Discussion

Clinical testing has revealed that oncolytic viral therapy is remarkably well tolerated, with minimal toxic effects attributable directly to the oncolytic virus [reviewed in (10,32)]. However, the efficacy of oncolytic virus therapy in patients has not yet been demonstrated. Tumor vasculature is a critical determinant of both tumor progression and its response to therapy (33,34). We hypothesized that changes in the tumor vasculature might influence the therapeutic efficacy of oncolytic virus treatment. Here, we have demonstrated that oncolytic virus treatment of rat gliomas is associated with a statistically significant increase in the permeability of the tumor vasculature. Our results further indicate that this oncolytic virus treatment–associated hyperpermeability of the tumor vasculature was associated with statistically significant increases in tumor inflammation and leukocyte infiltration. Furthermore, we found that pretreatment of gliomas with the angiogenesis inhibitor cRGD peptide reduced inflammation, vascular hyperpermeability, and leukocyte infiltration of tumor tissue upon treatment with oncolytic virus. Reduction of host immune responses by cRGD treatment also enhanced the anticancer efficacy of oncolytic virus treatment by increasing oncolytic virus propagation in tumors.

The vascular endothelium is an important component of the host inflammatory response that dictates the changes in host immune responses during inflammation (35). Peripheral leukocytes and mononuclear cells constantly circulate within blood vessels, where they remain ready to initiate host defense mechanisms in response to injury or infection. During inflammation, these cells extravasate into the tissue via a sequential process that is initiated by their adhesion to the endothelial cells that line the vascular walls, which leads to endothelial cell activation. Activated endothelium is characterized by vascular hyperpermeability and increased tissue edema, which facilitate perivascular inflammatory cell infiltration (28,35). We hypothesized that the highly angiogenic nature of tumors increases the area of vascularity, which may in turn exacerbate oncolytic virus–induced inflammation. The key role played by blood vessels in increasing tissue inflammation is bolstered by the observation that increased microvessel density in transgenic mice engineered to overexpress VEGF-A led to a statistically significantly increased and prolonged inflammatory response compared with wild-type mice. Notably, this exaggerated inflammatory response could be blocked by antibodies against the VEGF-A receptor, VEGFR-2 (26). Similarly, overexpression of angiogenic placental growth factor has been associated with pronounced vascular enlargement and increased swelling, edema, and leukocyte infiltration (36). Together these studies underscore the critical role played by angiogenesis in inflammation. Here, we tested the role of the tumor endothelium in oncolytic virus therapy by testing changes in vascular perfusion upon oncolytic virus treatment of tumors. Our results have uncovered a statistically significant increase in vascular permeability, tissue inflammation, and leukocyte infiltration in oncolytic virus–treated tumor tissue compared with PBS-treated control tumors.

Increased infiltration of host innate immune cells in response to oncolytic virus infection is thought to be primarily responsible for the rapid clearance of virus from tumors (21,37,38). Cyclophosphamide treatment of rats with brain tumors has been previously shown to enhance therapeutic efficacy of oncolytic virus treatment in vivo (17). The active metabolites of cyclophosphamide can also induce cell killing by induction of apoptosis, leading to a direct anticancer effect (39). However, the active metabolites of cyclophosphamide are restricted from crossing the blood–brain barrier, and only subtherapeutic levels of cyclophosphamide are achieved in brain tissue after systemic administration (40).

Moreover, addition of an active metabolite of cyclophosphamide directly to cancer cells in vitro leads to inhibition of oncolytic virus replication, which is in direct contrast to the enhanced oncolytic virus replication observed in vivo (17). In addition, cyclophosphamide is able to augment the antitumor efficacy of oncolytic virus therapy only when given as a pretreatment and not when administered after oncolytic virus treatment (11,12,17). We (11,12,17) and others (23–25,41,42) have reported that transient suppression of host immune responses by systemic cyclophosphamide treatment of tumor-bearing animals enhances the therapeutic efficacy of oncolytic viruses by limiting the infiltration of inflammatory cells into tumor tissue and increasing viral replication. In this study, we also confirmed these previous findings by demonstrating that cyclophosphamide treatment suppressed host inflammatory responses and supported increased oncolytic virus presence in tumors. More interesting, we tested the effect of cyclophosphamide treatment on oncolytic virus–induced vascular leakage. Tumors harvested from rats treated with cyclophosphamide did not display vascular hyperpermeability in response to oncolytic virus infection. Together, these results indicate that the vascular leakage we observed in tumor tissue was closely linked to inflammation and was in response to oncolytic virus infection of tumors.

Angiostatic agents such as thrombospondin-2, vasostatin, angiostatin, and anti-VEGF antibodies have been shown to reduce vascular leakage, edema, and experimental inflammation (26,27,43–45). Hence, we hypothesized that it might be possible to use antiangiogenic agents to limit oncolytic virus–induced tumor inflammation. We tested the effect of cRGD peptide, a known antagonist for vitronectin binding to cell-surface integrins $\alpha_v\beta_3$, and $\alpha_v\beta_5$, which are highly expressed on proliferating endothelial cells. Blocking integrin ligation has been shown to be a potent inhibitor of angiogenesis and glioma growth in vivo (13,30). More recently, cRGD treatment of rats with middle cerebral artery occlusion was shown to preserve the blood–brain and ameliorate focal cerebral ischemic damage by reducing vascular leakage and edema (46). Our data show that pretreatment with cRGD peptide in conjunction with oncolytic virus therapy statistically significantly enhanced the therapeutic efficacy of oncolytic virus treatment by reducing tumor microvessel density and reducing rapid viral clearance from the tissue. It is interesting that cyclophosphamide has also been shown to have an antiangiogenic effect on tumors in vivo (47). In future studies, it would be interesting to investigate the contribution of antiangiogenic effect of cyclophosphamide treatment in enhancement of oncolytic virus efficacy in vivo.

To evaluate if changes in vascular leakage were associated with tissue inflammation, we examined changes in the expression of genes encoding chemokines (and their receptors) that are known mediators of the inflammatory response in oncolytic virus–treated tumor tissue. Among the genes whose expression changed by more than twofold in oncolytic virus–treated tumor tissue compared with PBS-treated tumors, the IFN-γ gene and IFN-γ–induced genes such as CXCL11 and CXCL9 (48) displayed statistically significantly increased expression. Notably, these genes also displayed decreased expression in tumor tissue that was pretreated with cRGD peptide before oncolytic virus therapy compared with tumors treated with PBS before oncolytic therapy. IFN-γ has also been shown to increase vascular permeability (49). We found that tumors pretreated with cRGD peptide before oncolytic virus infection had reduced levels of IFN-γ, CXCL9, and CXCL 11 compared with tumors from rats treated with oncolytic virus alone. These results suggest that increased expression of IFN-γ, which is a key modulator of host responses to oncolytic viruses (31), is attenuated by antiangiogenic pretreatment of tumors before oncolytic virus–induced inflammatory response.

It is becoming increasingly apparent that the future of cancer treatment lies in the rational combination of drugs that target different aspects of tumor biology to enhance therapeutic benefit. Tumors treated with DNA-damaging chemotherapeutic agents, such as temozolomide and cisplatin, often develop resistance by activating cellule DNA–repair pathway. However, the induction of these DNA repair pathways provides a better environment for virus replication and hence synergizes with oncolytic virus therapy (50,51). Treatment with ionizing radiation also induces changes in gene expression and in posttranslational modifications of cellular proteins that enhance the efficacy of oncolytic viruses (52). Treatment with antiangiogenic agents can lead to an initial trimming down of aberrant tumor blood vessels. This reduction in blood vessel density reduces vascular leakage, interstitial pressure, and also results in improved tumor circulation with reduced tumor hypoxia (9,53). This antiangiogenic agent–mediated trimming down of tumor blood vessels, which is also referred to as vascular normalization, allows for better tumor oxygenation and spread of therapeutic molecules which is exploited to enhance efficacy of radiation and chemotherapy (53,54). To our knowledge, this is the first study to demonstrate that suppression of host immune responses to oncolytic virus therapy can be achieved with single treatment of an angiostatic agent, resulting in the enhanced efficacy of oncolytic virus therapy of tumors. In addition, the anti-inflammatory effect of cRGD treatment was localized to tumor and no statistically significant change in the expression of inflammatory cytokines and their receptors was observed in peripheral blood mononuclear cells of rats treated with cRGD before oncolytic virus compared with oncolytic virus–treated rats alone (data not shown). This finding suggested that cRGD peptide pretreatment of tumors before oncolytic viral therapy could enhance oncolytic virus efficacy without producing the potential immunosuppressive toxic effects that are associated with chemotherapy. Finally, the increased viral replication supported by tumors treated with cRGD peptide may enable reduction of oncolytic virus dosage needed to observe an antitumor response.

This study has several limitations. First, the enhanced efficacy of oncolytic viral therapy by cRGD peptide pretreatment was observed in a rat syngeneic glioma model. It would be interesting to extend these finding to human glioma models in athymic nude mice to establish the generalizability of the effect. Second, the increased viral replication supported by tumors pretreated with cRGD peptide could lead to toxic effects that are associated with increased viral burden. However, rats and mice are resistant to HSV infection, and so future toxicity studies in primate models would be necessary to evaluate the toxicity of this combination regimen. Finally, a careful study evaluating the systemic delivery of cRGD

peptide and escalating dosage schedules of this antiangiogenic drug in combination with multiple different oncolytic viruses would be essential to optimize this treatment regimen.

This study provides a paradigm for the treatment of tumors using antiangiogenic agents in combination with oncolytic virus. Additional studies will be needed to demonstrate the feasibility of a multimodal treatment approach that combines antiangiogenic agents, radiation, chemotherapeutics, and oncolytic virus therapy to destroy glioma.

References

(1) Norton L, Massague J. Is cancer a disease of self-seeding? Nat Med 2006;12:875–8.

(2) Jain RK, Duda DG, Clark JW, Loeffler JS. Lessons from phase III clinical trials on anti-VEGF therapy for cancer. Nat Clin Pract Oncol 2006;3: 24–40.

(3) Penas-Prado M, Gilbert MR. Molecularly targeted therapies for malignant gliomas: advances and challenges. Expert Rev Anticancer Ther 2007;7: 641–61.

(4) Folkman J. Tumor angiogenesis: therapeutic implications. N Engl J Med 1971;285:1182–6.

(5) Aghi M, Cohen KS, Klein RJ, Scadden DT, Chiocca EA. Tumor stromal-derived factor-1 recruits vascular progenitors to mitotic neovasculature, where microenvironment influences their differentiated phenotypes. Cancer Res 2006;66:9054–64.

(6) Abe T, Terada K, Wakimoto H, Inoue R, Tyminski E, Bookstein R, et al. PTEN decreases in vivo vascularization of experimental gliomas in spite of proangiogenic stimuli. Cancer Res 2003;63:2300–5.

(7) Brat DJ, Kaur B, Van Meir EG. Genetic modulation of hypoxia induced gene expression and angiogenesis: relevance to brain tumors. Front Biosci 2003;8:D100–16.

(8) Kaur B, Khwaja FW, Severson EA, Matheny SL, Brat DJ, Van Meir EG. Hypoxia and the hypoxia-inducible-factor pathway in glioma growth and angiogenesis. Neuro Oncol 2005;7:134–53.

(9) Jain RK. Normalization of tumor vasculature: an emerging concept in antiangiogenic therapy. Science 2005;307:58–62.

(10) Cutter JL, Kurozumi K, Chiocca EA, Kaur B. Gene therapeutics: the future of brain tumor therapy? Expert Rev Anticancer Ther 2006;6:1053–64.

(11) Fulci G, Breymann L, Gianni D, Kurozomi K, Rhee SS, Yu J, et al. Cyclophosphamide enhances glioma virotherapy by inhibiting innate immune responses. Proc Natl Acad Sci USA 2006;103:12873–8.

(12) Lamfers ML, Fulci G, Gianni D, Tang Y, Kurozumi K, Kaur B, et al. Cyclophosphamide increases transgene expression mediated by an oncolytic adenovirus in glioma-bearing mice monitored by bioluminescence imaging. Mol Ther 2006;14:779–88.

(13) Yamada S, Bu XY, Khankaldyyan V, Gonzales-Gomez I, McComb JG, Laug WE. Effect of the angiogenesis inhibitor Cilengitide (EMD 121974) on glioblastoma growth in nude mice. Neurosurgery 2006;59:1304–12; discussion 1312.

(14) Nabors LB, Mikkelsen T, Rosenfeld SS, Hochberg F, Akella NS, Fisher JD, et al. Phase I and correlative biology study of cilengitide in patients with recurrent malignant glioma. J Clin Oncol 2007;25:1651–7.

(15) Goldstein DJ, Weller SK. Herpes simplex virus type 1-induced ribonucleotide reductase activity is dispensable for virus growth and DNA synthesis: isolation and characterization of an ICP6 lacZ insertion mutant. J Virol 1988;62:196–205.

(16) Terada K, Wakimoto H, Tyminski E, Chiocca EA, Saeki Y. Development of a rapid method to generate multiple oncolytic HSV vectors and their in vivo evaluation using syngeneic mouse tumor models. Gene Ther 2006;13:705–14.

(17) Wakimoto H, Fulci G, Tyminski E, Chiocca EA. Altered expression of antiviral cytokine mRNAs associated with cyclophosphamide's enhancement of viral oncolysis. Gene Ther 2004;11:214–23.

(18) Narita Y, Nagane M, Mishima K, Huang HJ, Furnari FB, Cavenee WK. Mutant epidermal growth factor receptor signaling down-regulates p27 through activation of the phosphatidylinositol 3-kinase/Akt pathway in glioblastomas. Cancer Res 2002;62:6764–9.

(19) Kambara H, Okano H, Chiocca EA, Saeki Y. An oncolytic HSV-1 mutant expressing ICP34.5 under control of a nestin promoter increases survival of animals even when symptomatic from a brain tumor. Cancer Res 2005;65:2832–9.

(20) Cui X, Churchill GA. Statistical tests for differential expression in cDNA microarray experiments. Genome Biol 2003;4:210.

(21) Davis JJ, Fang B. Oncolytic virotherapy for cancer treatment: challenges and solutions. J Gene Med 2005;7:1380–9.

(22) Millan J, Ridley AJ. Rho GTPases and leucocyte-induced endothelial remodelling. Biochem J 2005;385(Pt 2):329–37.

(23) Eiselein JE, Biggs MW, Walton JR. Treatment of transplanted murine tumors with an oncolytic virus and cyclophosphamide. Cancer Res 1978;38(Pt 1):3817–22.

(24) Di Paolo NC, Tuve S, Ni S, Hellstrom KE, Hellstrom I, Lieber A. Effect of adenovirus-mediated heat shock protein expression and oncolysis in combination with low-dose cyclophosphamide treatment on antitumor immune responses. Cancer Res 2006;66:960–9.

(25) Jooss K, Yang Y, Wilson JM. Cyclophosphamide diminishes inflammation and prolongs transgene expression following delivery of adenoviral vectors to mouse liver and lung. Hum Gene Ther 1996;7:1555–66.

(26) Kunstfeld R, Hirakawa S, Hong YK, Schacht V, Lange-Asschenfeldt B, Velasco P, et al. Induction of cutaneous delayed-type hypersensitivity reactions in VEGF-A transgenic mice results in chronic skin inflammation associated with persistent lymphatic hyperplasia. Blood 2004;104: 1048–57.

(27) Park YW, Kang YM, Butterfield J, Detmar M, Goronzy JJ, Weyand CM. Thrombospondin 2 functions as an endogenous regulator of angiogenesis and inflammation in rheumatoid arthritis. Am J Pathol 2004;165: 2087–98.

(28) Jackson JR, Seed MP, Kircher CH, Willoughby DA, Winkler JD. The codependence of angiogenesis and chronic inflammation. FASEB J 1997; 11:457–65.

(29) Rosales C, Juliano RL. Signal transduction by cell adhesion receptors in leukocytes. J Leukoc Biol 1995;57:189–98.

(30) MacDonald TJ, Taga T, Shimada H, Tabrizi P, Zlokovic BV, Cheresh DA, et al. Preferential susceptibility of brain tumors to the antiangiogenic effects of an alpha(v) integrin antagonist. Neurosurgery 2001;48: 151–7.

(31) Pierce AT, DeSalvo J, Foster TP, Kosinski A, Weller SK, Halford WP. Beta interferon and gamma interferon synergize to block viral DNA and virion synthesis in herpes simplex virus-infected cells. J Gen Virol 2005;86:2421–32.

(32) Aghi M, Martuza RL. Oncolytic viral therapies—the clinical experience. Oncogene 2005;24:7802–16.

(33) Folkman J. Role of angiogenesis in tumor growth and metastasis. Semin Oncol 2002;29 Suppl 16:15–8.

(34) van Kempen LC, Ruiter DJ, van Muijen GN, Coussens LM. The tumor microenvironment: a critical determinant of neoplastic evolution. Eur J Cell Biol 2003;82:539–48.

(35) Frantz S, Vincent KA, Feron O, Kelly RA. Innate immunity and angiogenesis. Circ Res 2005;96:15–26.

(36) Oura H, Bertoncini J, Velasco P, Brown LF, Carmeliet P, Detmar M. A critical role of placental growth factor in the induction of inflammation and edema formation. Blood 2003;101:560–7.

(37) Chiocca EA, Abbed KM, Tatter S, Louis DN, Hochberg FH, Barker F, et al. A phase I open-label, dose-escalation, multi-institutional trial of injection with an E1B-attenuated adenovirus, ONYX-015, into the peritumoral region of recurrent malignant gliomas, in the adjuvant setting. Mol Ther 2004;10:958–66.

(38) Pecora AL, Rizvi N, Cohen GI, Meropol NJ, Sterman D, Marshall JL, et al. Phase I trial of intravenous administration of PV701, an oncolytic virus, in patients with advanced solid cancers. J Clin Oncol 2002;20: 2251–66.

(39) Schwartz PS, Waxman DJ. Cyclophosphamide induces caspase 9-dependent apoptosis in 9L tumor cells. Mol Pharmacol 2001;60: 1268–79.

(40) Genka S, Deutsch J, Stahle PL, Shetty UH, John V, Robinson C, et al. Brain and plasma pharmacokinetics and anticancer activities of cyclophosphamide and phosphoramide mustard in the rat. Cancer Chemother Pharmacol 1990;27:1–7.
(41) Smakman N, van der Bilt JD, van den Wollenberg DJ, Hoeben RC, Borel Rinkes IH, Kranenburg O. Immunosuppression promotes reovirus therapy of colorectal liver metastases. Cancer Gene Ther 2006;13:815–8.
(42) Ikeda K, Ichikawa T, Wakimoto H, Silver JS, Deisboeck TS, Finkelstein D, et al. Oncolytic virus therapy of multiple tumors in the brain requires suppression of innate and elicited antiviral responses. Nat Med 1999;5: 881–7.
(43) Lange-Asschenfeldt B, Weninger W, Velasco P, Kyriakides TR, von Andrian UH, Bornstein P, et al. Increased and prolonged inflammation and angiogenesis in delayed-type hypersensitivity reactions elicited in the skin of thrombospondin-2–deficient mice. Blood 2002;99:538–45.
(44) Pike SE, Yao L, Jones KD, Cherney B, Appella E, Sakaguchi K, et al. Vasostatin, a calreticulin fragment, inhibits angiogenesis and suppresses tumor growth. J Exp Med 1998;188:2349–56.
(45) Su G, Hodnett M, Wu N, Atakilit A, Kosinski C, Godzich M, et al. Integrin {alpha}v{beta}5 regulates lung vascular permeability and pulmonary endothelial barrier function. Am J Respir Cell Mol Biol 2006;36: 377–86.
(46) Shimamura N, Matchett G, Yatsushige H, Calvert JW, Ohkuma H, Zhang J. Inhibition of integrin alphavbeta3 ameliorates focal cerebral ischemic damage in the rat middle cerebral artery occlusion model. Stroke 2006;37:1902–9.
(47) Browder T, Butterfield CE, Kraling BM, Shi B, Marshall B, O'Reilly MS, et al. Antiangiogenic scheduling of chemotherapy improves efficacy against experimental drug-resistant cancer. Cancer Res 2000;60:1878–86.
(48) Kanda N, Watanabe S. Prolactin enhances interferon-gamma-induced production of CXC ligand 9 (CXCL9), CXCL10, and CXCL11 in human keratinocytes. Endocrinology 2007;148:2317–25.
(49) Martin S, Maruta K, Burkart V, Gillis S, Kolb H. IL-1 and IFN-gamma increase vascular permeability. Immunology 1988;64:301–5.
(50) Aghi M, Rabkin S, Martuza RL. Effect of chemotherapy-induced DNA repair on oncolytic herpes simplex viral replication. J Natl Cancer Inst 2006;98:38–50.
(51) Adusumilli PS, Chan MK, Chun YS, Hezel M, Chou TC, Rusch VW, et al. Cisplatin-induced GADD34 upregulation potentiates oncolytic viral therapy in the treatment of malignant pleural mesothelioma. Cancer Biol Ther 2006;5:48–53.
(52) Advani SJ, Mezhir JJ, Roizman B, Weichselbaum RR. ReVOLT: radiation-enhanced viral oncolytic therapy. Int J Radiat Oncol Biol Phys 2006;66:637–46.
(53) Winkler F, Kozin SV, Tong RT, Chae SS, Booth MF, Garkavtsev I, et al. Kinetics of vascular normalization by VEGFR2 blockade governs brain tumor response to radiation: role of oxygenation, angiopoietin-1, and matrix metalloproteinases. Cancer Cell 2004;6:553–63.
(54) Ma J, Li S, Reed K, Guo P, Gallo JM. Pharmacodynamic-mediated effects of the angiogenesis inhibitor SU5416 on the tumor disposition of temozolomide in subcutaneous and intracerebral glioma xenograft models. J Pharmacol Exp Ther 2003;305:833–9.

Funding

The National Brain Tumor Foundation, Glioblastoma Multiforme Grant (to B. K.); National Institutes of Health Grant (P01 CA069246 to F. H. H, E. A. C, and R. W.); American Association for Neurological Surgeons/Congress of Neurological Surgeons, Section on Tumors/BrainLab International Research Fellowship (to K. K.).

Notes

We thank Rosalyn Uhrig for help with manuscript preparation. The sponsors had no role in the design of the study; the collection, analysis, or interpretation of the data; the writing of the manuscript; or the decision to submit the manuscript for publication.

Manuscript received January 30, 2007; revised September 17, 2007; accepted October 18, 2007.